JOURNAL OF SPACECRAFT AND ROCKETS
Vol. 38, No. 3, May–June 2001

Plume Mass Spectrometry with a Hydrazine Arcjet Thruster

James E. Pollard*
The Aerospace Corporation, Los Angeles, California 90009
Ideo Masuda†
National Space Development Agency, Ibaraki 305-8505, Japan
and
Yoshifumi Gotoh‡
Mitsubishi Electric Corporation, Kanagawa 247, Japan

Molecular beam mass spectrometry was used to measure the chemical composition, angular distribution, and speed distribution in the plume of an arcjet thruster at 127 mm from the nozzle. The arcjet operating conditions were 1660 W of input power, 46.4 mg/s of simulated hydrazine propellant, and a background pressure of 0.85 mtorr. Time-of-flight spectra yielded speed distributions for N_2, N, H_2, and H as a function of angle θ relative to plume centerline. Absolute fluxes were obtained from the experimental relative flux distributions by normalizing to the total mass flow rate. Dissociation fractions for N_2 and H_2 were 11 and 14%. Molecules near the centerline had most probable speeds of 7.4 km/s with the high end of the distribution extending to 10–12 km/s. The N_2 speed decreased to 2.7 km/s at $\theta = 80$ deg. The N_2 and N accounted for 89% of the arcjet thrust, and the mass flux for both species decreased by a factor of 10^4 between $\theta = 0$ and 90 deg. The angular distributions of H_2 and H were much broader, with mass fluxes that decreased by less than a factor of 10 between $\theta = 0$ and 90 deg. Other quantities derived from time-of-flight spectra were the momentum flux, kinetic power flux, average speed, and translational temperature.

Nomenclature

F	=	thrust, N
f	=	mass flux, $\mathrm{kg \cdot s^{-1} \cdot sr^{-1}}$
M	=	molar weight, $\mathrm{kg \cdot mol^{-1}}$
N	=	number density, $\mathrm{m^{-3}}$
p	=	momentum flux, $\mathrm{N \cdot sr^{-1}}$
R	=	gas constant, 8.314510 $\mathrm{J\ mol^{-1} \cdot K^{-1}}$
r	=	distance from source, m
S	=	mass spectrometer signal, V
S_x	=	detection sensitivity for species x, dimensionless
T_s	=	stream temperature, K
T_{tr}	=	translational temperature, K
t	=	time, s
v	=	velocity, $\mathrm{m\ s^{-1}}$
v_s	=	stream velocity, $\mathrm{m\ s^{-1}}$
w	=	kinetic power flux, $\mathrm{W \cdot sr^{-1}}$
θ	=	polar angle relative to plume centerline, deg or rad

Introduction

DATA relay test satellites (DRTS) are being developed by Mitsubishi Electric Corporation and National Space Development Agency of Japan. Hydrazine arcjet thrusters manufactured by PRIMEX Aerospace Company (PAC) will be used on DRTS for north–south stationkeeping.[1,2] Four arcjets are mounted on the north panel of the spacecraft, and they are fired in pairs for approximately half an hour, three times per week to control the orbit inclination and right ascension. Laboratory measurements and mathematical modeling were performed to assess the attitude disturbances, orbit perturbations, and thermal loading caused by plume impingement. This paper describes an investigation of the plume using molecular beam mass spectrometry. To our knowledge, there is no previous use of this technique for a flight-model arcjet at the level of detail to be presented here. In a complementary study, the flow near the exit plane was examined nonintrusively by laser-induced fluorescence.[3] The measurements allow optimization of direct simulation Monte Carlo (DSMC) input parameters (in particular, the chemical composition and nozzle temperature) and validation of the model for the DRTS application.[4]

Arcjet Operation

The MR 509-A/B arcjet is operated in a diffusion-pumped, 30-$\mathrm{m^3}$, stainless-steel vacuum tank as was done in our previous arcjet experiments,[5] using a certified ultrahigh-purity gas mixture containing mole fractions of 67.3% H_2 and 32.7% N_2 (nominally 2:1). Except for removing the catalytic gas generator, the arcjet thruster, power cable, and power processor are equivalent to DRTS flight hardware. The mass flow rate and inlet gas density are nearly the same for our mixture as for decomposed N_2H_4, but the inlet temperature is 300–350 K rather than 700–800 K. Decomposed N_2H_4 contains NH_3 in an amount that depends on temperature and pressure, but dissociation of NH_3 in the arc-heated nozzle means that it would be a minor constituent of plume. Based on previous measurements by NASA and PAC,[6] the 2:1 $H_2 + N_2$ gas mixture at ambient temperature is expected to reduce the thrust and specific impulse by 2% compared with decomposed N_2H_4 at the same flow rate, for example, 504 s specific impulse rather than 514 s. The reproducibility and accuracy of the mass flow settings are better than $\pm 1\%$, that is, ± 0.5 mg/s at 50 mg/s flow rate. Tests are performed at 1660 W of input power with four flow rates that are representative of arcjet operation on the DRTS spacecraft, as listed in Table 1. Unless stated otherwise, the results presented here are for the nominal flow rate of 46.4 mg/s.

Mass Spectrometry Apparatus

The thruster is mounted on a computer-controlled rotary platform for exploring the angular range between $\theta = 0$ and 100 deg. As shown in Fig. 1, the rotation axis is aligned with the arcjet exit plane. A complete map of the plume velocity vector distribution in the far field for each species can be obtained from scans of the polar angle θ, provided that the flow is axisymmetric. The copper skimmer has an orifice diameter of 2.0 mm, a height of 49 mm, an internal angle of 45 deg, and an external angle of 60 deg. To dissipate the major portion of the plume heat load, a water-cooled copper plate is attached to the bulkhead on which the skimmer is mounted. Plume data are recorded with the skimmer orifice 127 mm downstream of

Received 29 May 2000; revision received 4 October 2000; accepted for publication 9 October 2000.

*Senior Scientist, Space Materials Laboratory, P.O. Box 92957-M5/754.
†Assistant Senior Engineer, Data Relay Test Satellite Project Team, 2-1-1 Sengen, Tsukuba.
‡Senior Engineer, Space Systems Department, 325, Kamimachiya Kamakura.

Table 1 Operating parameters for the MR 509-A/B arcjet using a 2:1 mixture of $H_2 + N_2$

Flow rate, mg/s	Facility pressure, mtorr	Arc voltage, V	Arc current, A	Thrust, mN[a]	Specific impulse, s[a]	Thrust power, W[a]
43.1	0.79	102.3	16.2	220	524	565
46.4[b]	0.85	105.1	15.8	230	514	580
49.6	0.91	109.1	15.2	239	503	589
62.7[b]	1.17	120.5	13.8	278	462	630

[a]Beginning-of-life performance estimated from PRIMEX thrust stand data.[1]
[b]Nominal flow is 46.4 mg/s; high flow is 62.7 mg/s.

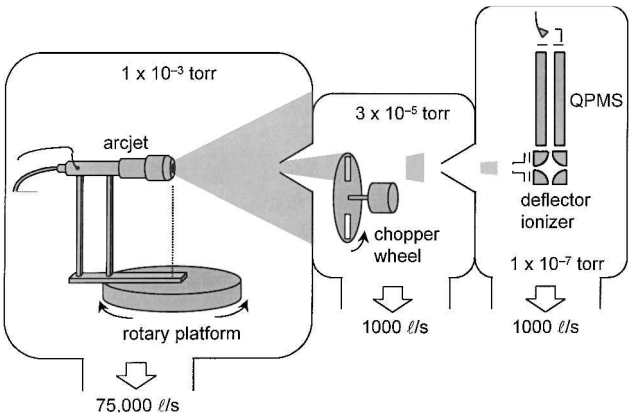

Fig. 1 Apparatus for measuring angular and speed distributions of plume molecules.

the arcjet exit plane, which was selected in the following way.[7] A nozzle-to-skimmer distance less than 90 mm decreases the signal near the plume centerline because the incident flow encounters an increasing density of reflected gas at the skimmer orifice. This undesirable situation is exemplified by a dip in the N_2 angular distribution near centerline. The hot-flow gas mixture is much less susceptible to this effect than is the same mixture at cold flow because the scattering cross section decreases at higher velocity[8] and because the increased forward momentum of the incident particles is relatively less altered by collisions with slowly moving targets. Increasing the nozzle-to-skimmer distance beyond 130 mm gradually decreases the signal due to attenuation by the background gas. The nozzle-to-skimmer distance is chosen to be slightly greater than the distance that maximizes the centerline signal as a compromise between skimmer interference and background gas attenuation of the plume.

Background pressure is measured by a capacitance manometer on the forward bulkhead at 0.8 m from the skimmer, and it is maintained at 0.85 mtorr by diffusion pumps with a combined speed of 75,000 l/s, as measured for 2:1 $H_2 + N_2$ at cold flow. A key requirement for plume mass spectrometry is that the background pressure be low enough to perturb minimally the flow within the probe volume at 100–150 mm from the nozzle. Collisions between the plume molecules and background species are unavoidable, but they are of little consequence in the higher density region near the nozzle, where they are outnumbered by collisions between plume molecules. Plume/background scattering becomes an issue when the density of the flow decreases to that of the background. The distance from the nozzle where this condition occurs is 140–240 mm for $\theta = 0$ deg, 80–130 mm for $\theta = 30$ deg, and 20–30 mm for $\theta = 90$ deg, according to the DSMC calculations.[4] We estimate the probability of elastic scattering of plume species in the region where the background density exceeds that of the plume, based on an extrapolation of the cross sections measured at ambient temperature to the higher velocities in the plume ($\sigma \propto v^{-0.182}$) (Ref. 8). One further assumption is that only the N_2 and N in the background cause significant deflection of N_2 and N in the plume, whereas H_2 and H in the plume are scattered by all background species. For N_2 and N, the scattering probability ranges from 1% at $\theta = 30$ deg to 23% at $\theta = 90$ deg and, for H_2 and H, the probability ranges from 28% at $\theta = 30$ deg to 53% at $\theta = 90$ deg. These probabilities include all possible elastic collisions between real molecules, that is, not hard spheres, the majority of which give deflection angles less than 20 deg (Ref. 8). We conclude that N_2 and N (the primary thrust carriers) are minimally affected by interaction with the background gas and that H_2 and H are perturbed to a measurable extent for $\theta \geq 30$ deg.

Plume molecules are detected by a quadrupole mass spectrometer (QPMS) that is optimized for the mass range below 30 atomic mass units (amu) and is equipped with an electron-impact deflector ionizer and a channel electron multiplier. The multiplier output is sent to a current preamplifier having a gain of 10 V/μA and a rise time of 10 μs. Waveform averaging of the time-of-flight (TOF) spectra for up to 10^4 shots enhances the signal-to-noise ratio at a given angle. To improve the detection sensitivity for H and N atoms, an electron-impact energy of 20 eV is chosen to minimize the extent of dissociative ionization, that is, $H_2 \rightarrow H^+ + H$ and $N_2 \rightarrow N^+ + N$. Figure 2 shows a mass spectrum (after background subtraction) recorded while admitting a small amount of the propellant mixture into the mass spectrometer through a leak valve. Here the N^+ production from N_2 is negligible compared to N_2^+, and the H^+/H_2^+ ratio from ionization of H_2 is only 1%. The spectrum in Fig. 3 is measured on the arcjet plume centerline using molecular beam sampling; it displays an H^+/H_2^+ ratio of 9%, along with signals at 14 (N), 15 (NH), 16 (NH_2), and 17 amu (NH_3) that are absent in Fig. 2. No time-correlated signal is seen at 17 amu when the wheel is spinning, and therefore, NH_3 is not a detectable constituent of the plume. However, the presence of time-correlated signals at 1, 14, 15, and 16 amu (in addition to the demonstrated minimal extent of dissociative ionization) proves that the sampling system can detect H, N, NH, and NH_2 in the plume.

The speed distribution of a collimated supersonic molecular beam is conventionally represented by

$$\frac{df}{dv} \propto v^3 \exp\left[\frac{-M(v - v_s)^2}{2RT_s}\right] \tag{1}$$

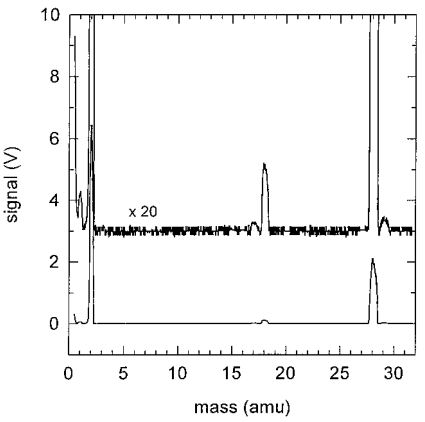

Fig. 2 Mass spectrum of the 2:1 $H_2 + N_2$ gas mixture using a leak valve to bleed the sample into the mass spectrometer vacuum chamber.

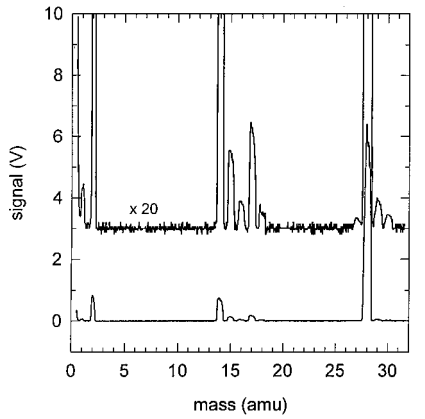

Fig. 3 Mass spectrum measured on plume centerline during arcjet operation using molecular beam sampling with the chopper wheel in the open position.

This applies to an idealized flow at the skimmer orifice that has a three-dimensional Maxwellian speed distribution at the stream temperature T_s superimposed on the stream flow velocity v_s (Refs. 9 and 10). Here df represents mass flow per steradian, that is, mass flux, in the speed increment dv. The arcjet flow differs from this idealized case, but our final results are independent of the assumptions underlying Eq. (1) because we use the equation only for least-squares fitting and not for extracting the average speed or translational temperature.

The chopper wheel has four 1.6-mm-wide slots and is rotated at 200 revolutions per second, giving a nominal shutter duration of 23 μs. Calibration of the speed measurements is performed by comparing TOF spectra for a cold flow of helium through the arcjet. A relatively short drift distance is chosen (583 mm from wheel to ionizer) to enhance the sensitivity and to enable the detection of plume species at high angles. As a consequence, it is necessary to account for the wheel shutter function when extracting the speed distribution from a TOF spectrum as follows. The molecular flux at the ionizer is assumed to be proportional to the mass flow per steradian df/dv at the skimmer as given by Eq. (1). The output signal S from the QPMS is proportional to the number density at the ionizer and, hence, S is proportional to molecular flux divided by v. The TOF spectrum dS/dt is then given by

$$\frac{dS}{dt} \propto \left|\frac{dv}{dt}\right| v^2 \exp\left[\frac{-M(v-v_s)^2}{2RT_s}\right] \tag{2}$$

This expression is convolved with the measured shutter function using fast Fourier transforms as part of the least-squares-fitting routine. Fitting of each TOF spectrum to the convolved Eq. (2) yields the parameters v_s and T_s. The routine gives a very good representation of the data in most cases, as shown in Figs. 4 and 5.

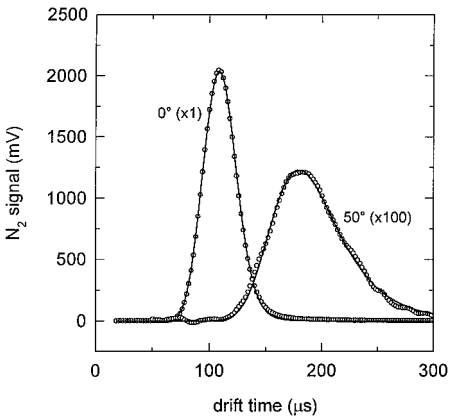

Fig. 4 TOF spectra for N_2 in the arcjet plume; data points and least-squares curves are shown at angles of $\theta = 0$ and 50 deg.

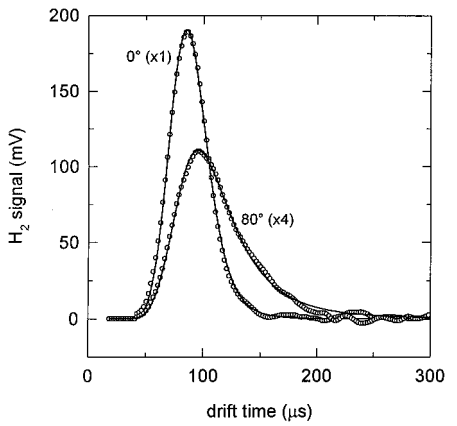

Fig. 5 TOF spectra for H_2 in the arcjet plume; data points and the least-squares curves are shown at angles of $\theta = 0$ and 80 deg.

Results and Discussion

TOF spectra for N_2, N, H_2, and H in the arcjet plume are recorded in 10-deg increments from $\theta = 0$ to 100 deg, and the data are converted to speed distributions. The area under the speed distribution curves as a function of angle (namely, the angular distribution) is multiplied by $\sin\theta$ to convert from flux per steradian to flux per radian for integration over the angular range. As a first approximation, this integral is proportional to the total flow rate of a given species in the plume. However, a correction factor is needed to account for the species-dependent apparatus sensitivity. The latter is needed to determine the amount of H relative to H_2 and the amount of N relative to N_2, but not for determining the overall ratio of plume hydrogen to nitrogen, which is specified by the propellant composition (67.3% H_2 + 32.7% N_2).

From published data,[11] N_2 and N have equal cross sections for electron-impact ionization at 20 eV, as do H_2 and H (all four cross sections are close to 3×10^{-17} cm^2 with an estimated uncertainty of $\pm 10\%$). Moreover, N_2 and N are observed to have similar angular distributions, as are H_2 and H. Therefore, we assume that N_2 and N in the plume are detected with equal sensitivity, S_{N2}, and that H_2 and H are detected with equal sensitivity, S_{H2}. Comparing integrated angular distributions for H_2 and N_2 gives a measured overall sensitivity ratio of $S_{H2}/S_{N2} = 0.629$. The measured sensitivity ratio of the QPMS for ambient temperature gases is $S_{H2}/S_{N2} = 1.48$, which means that the molecular beam sampling system enhances the detection of N_2 and N (relative to H_2 and H) by a factor of $1.48/0.629 = 2.35$. We present these observed ratios to illustrate the performance of the sampling system; they are not used as a correction for any of the data. Because the QPMS transmission varies by only a factor of 1.48 between masses that differ by a factor of 14, it is safe to assume that the QPMS transmission is approximately the same for masses that differ by a factor of 2, namely, H_2 and H or N_2 and N. The enhanced sensitivity of the sampling system for N_2 and N (relative to H_2 and H) is attributed to the larger source volume for H_2 and H, which gives greater nonparaxial velocity components at the skimmer and prevents a portion of the molecules from being detected.[5] In other words, the angular acceptance of the sampling system discriminates against molecules coming from the outer region of the extended source volume.

Based on the foregoing, dissociation fractions are calculated from the integrated angular distributions, and species flow rates are determined from the known total flow of hydrogen and nitrogen, with the results for nominal flow listed in Table 2. The main difference between nominal flow and high flow is that the dissociation fraction of N_2 decreases from 11 to 6%, as would be expected for a decrease in propellant specific energy (joules per kilogram). However, the H_2 dissociation fraction is 14% at both flow rates. A second data set recorded at nominal flow gives results similar to those in Table 2, with the addition of measurements for NH and NH_2, which have mole fractions of around 1.5 and 0.5% respectively.

Speed distributions measured over the angular range are plotted in Figs. 6 and 7 for N_2 and H_2 using Eq. (1) normalized to the mass flows in Table 2. Although the expected arcjet specific impulse corresponds to an average exhaust speed of about 5 km/s, molecules near the centerline have most probable speeds near 7.4 km/s, with the high end of the distribution extending up to 10–12 km/s. The most probable N_2 speed decreases to 2.8 km/s at angles away from the centerline. Speed distributions for H_2 are noticeably broader than for N_2, with a centerline peak at 7.9 km/s that decreases to 5.8 km/s at $\theta = 100$ deg. Integrating the speed distributions yields

Table 2 Plume chemical composition at nominal flow (46.4 mg/s) by mass spectrometry[a]

Species	Mole fraction	Dissociation fraction	Flow, mg/s
N_2	0.257	0.109 ± 0.013	36.0
N	0.063	——	4.4
H_2	0.510	0.143 ± 0.017	5.1
H	0.170	——	0.9

[a]Overall atom ratio of hydrogen to nitrogen is taken to be $67.3/32.7 = 2.06$.

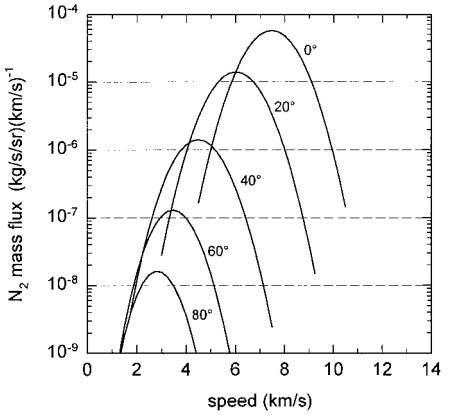

Fig. 6 Speed distributions for N_2.

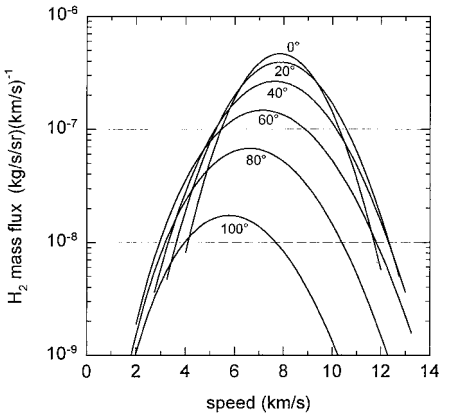

Fig. 7 Speed distributions for H_2.

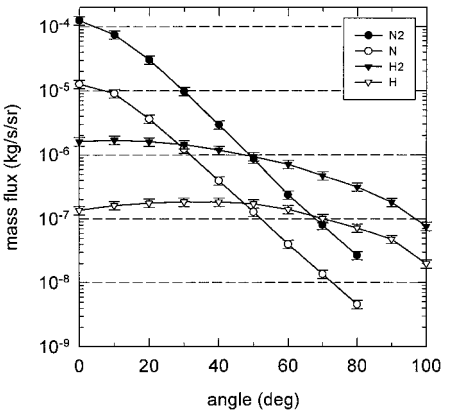

Fig. 8 Mass flux vs angle for N_2, N, H_2, and H.

the mass flow per steradian, that is, mass flux, as a function of angle shown in Fig. 8 for N_2, N, H_2, and H. The angular distributions are very similar for N_2 and N at a given flow rate, with the flux for both species decreasing by a factor of 10^4 between $\theta = 0$ and 90 deg. In previous measurements on the NASA modular arcjet with pure hydrogen propellant,[5] the H_2 mass flux decreased by a factor of 10^3 between 0 and 90 deg. However, in the present experiment with the 2:1 $H_2 + N_2$ gas mixture, the flux of H_2 and H decreases by less than a factor of 10 between 0 and 90 deg. We find that putting even a small amount of N_2 in the flow broadens the H_2 angular distribution, which suggests that H_2 is scattered more strongly by the heavy species than by other H_2 molecules.

A better understanding of scattering processes in the plume can be obtained by applying energy and momentum conservation to hard-sphere collisions between a fast projectile a slower target that is moving with the bulk flow velocity. We consider three cases: 1) For a light projectile and a heavy target, the initial velocity magnitudes are relatively unchanged by the collision, with the light species being scattered at angles anywhere between 0 and 180 deg and the heavy species continuing in the direction of the bulk flow. 2) For a heavy projectile and a light target, the heavy velocity change is small, and the light velocity change can be anywhere from zero up to a velocity greater than that of the projectile. The heavy scattering angle is kinematically restricted to a small value, for example, less than 4.1 deg for a 14:1 mass ratio, and the light scattering angle is restricted to a larger value, for example, between 47 and 90 deg for a 14:1 mass ratio. 3) Finally, for collisions between projectiles and targets of equal mass, both collision partners can undergo large velocity changes. Scattering angles are anywhere between 0 and 90 deg, and the angle between the two final velocity vectors must equal 90 deg.

Hence, in the large majority of collisions between species of different masses, the light molecule is deflected more than the heavy one. This mechanism explains the mass dependence of the plume angular distributions in Fig. 8. The case of a light projectile colliding with a heavy target is especially effective because the scattering angle can be as large as 180 deg. For H atoms in the arcjet plume, the scattering from N_2 and N is sufficient to yield a nearly isotropic distribution of H atoms over much of the angular range with the maximum flux occurring at 30 deg rather than on centerline. A closer look at Fig. 8 shows that N and H atoms have broader angular distributions than their respective parent molecules, as would be expected. One can also view trends seen here as an example of diffusive mass separation, which has been observed previously in freejet expansions at low Reynolds number.[12]

To derive the momentum flux, average speed, translational temperature, and speed ratio, we consider the number density speed distribution at a distance r from the source:

$$\frac{\mathrm{d}n}{\mathrm{d}v} = \frac{1}{Mr^2 v}\frac{\mathrm{d}f}{\mathrm{d}v} \tag{3}$$

The number density N at a distance r and angle θ is

$$N(r,\theta) = \int_0^\infty \frac{\mathrm{d}n}{\mathrm{d}v}\,\mathrm{d}v \tag{4}$$

The expectation value of v to the mth power is

$$\langle v'''\rangle = \frac{1}{N}\int_0^\infty \frac{\mathrm{d}n}{\mathrm{d}v} v'''\,\mathrm{d}v \tag{5}$$

The mass flux f, momentum flux p, and kinetic power flux w at an angle θ are

$$f(\theta) = \int_0^\infty \frac{\mathrm{d}f}{\mathrm{d}v}\,\mathrm{d}v = NMr^2\langle v\rangle \tag{6}$$

$$p(\theta) = \int_0^\infty \frac{\mathrm{d}f}{\mathrm{d}v} v\,\mathrm{d}v = NMr^2\langle v^2\rangle \tag{7}$$

$$w(\theta) = \frac{1}{2}\int_0^\infty \frac{\mathrm{d}f}{\mathrm{d}v} v^2\,\mathrm{d}v = \frac{1}{2}NMr^2\langle v^3\rangle \tag{8}$$

The net thrust F is the integral of $p\cos\theta$ over the forward hemisphere:

$$F = 2\pi\int_0^{\pi/2} p(\theta)\cos(\theta)\sin(\theta)\,\mathrm{d}\theta \tag{9}$$

The translational temperature T_{tr} is calculated by assuming the thermal energy associated with gas flow along the viewing axis is

$$\tfrac{1}{2}RT_{\mathrm{tr}} = \tfrac{1}{2}M\langle[v - \langle v\rangle]^2\rangle \tag{10}$$

which yields

$$T_{\mathrm{tr}} = (M/R)[\langle v^2\rangle - \langle v\rangle^2] \tag{11}$$

Table 3 Thrust determined by mass spectrometry at nominal flow (46.4 mg/s)

Species	Thrust, mN	Thrust fraction
N_2	209 ± 31	0.785
N	28 ± 4	0.104
H_2	25 ± 4	0.094
H	4 ± 1	0.017
Total	266 ± 40	1.000
PAC Total[a]	230 ± 5	——

[a]Beginning-of-life performance estimated from PRIMEX thrust stand data.[1]

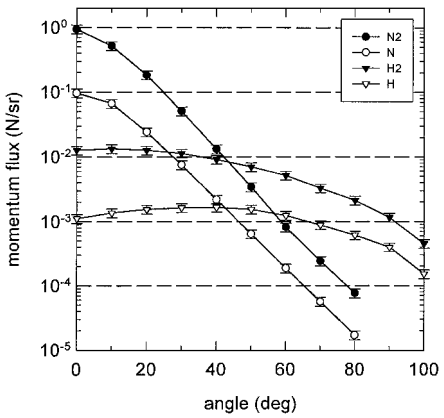

Fig. 9 Momentum flux vs angle for N_2, N, H_2, and H.

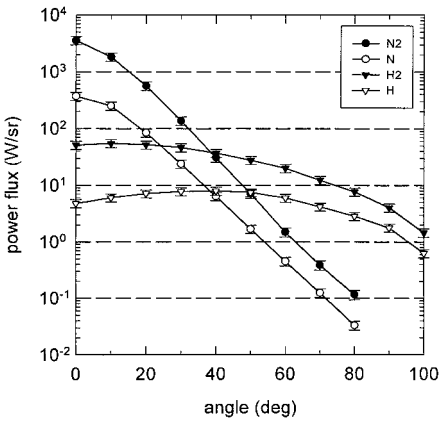

Fig. 10 Kinetic power flux vs angle for N_2, N, H_2, and H.

Error bars for these quantities in Figs. 8–12 are estimated systematic uncertainties associated with the apparatus calibration. Statistical uncertainties from the curve fitting are generally much smaller.

Momentum flux is a key parameter for evaluating plume impingement, and it is plotted as a function of angle in Fig. 9. For $\theta < 40$ deg, the momentum flux is dominated by N_2, whereas for $\theta > 50$ deg, the main contributor is H_2. Momentum flux is about 1 N/sr on the centerline, decreasing to 10^{-3} N/sr at $\theta = 90$ deg. The net thrust for each species from Eq. (9) is listed in Table 3. Here N_2 contributes 78.5% of the net thrust at nominal flow and 84.5% at high flow, while the contribution of N drops from 10.4 to 6.2% when the flow is increased. There is an 8–9% contribution to net thrust from H_2 and less than a 2% contribution from H. Comparing our total thrust in Table 3 with the values derived from PAC thrust stand data indicates an overall accuracy of ±10–15%. Of course, the main purpose of this experiment is not to determine thrust, but to measure the plume chemical composition, angular distribution, and speed distribution.

The kinetic power flux plotted as a function of angle in Fig. 10 provides a measure of the convective heat input on spacecraft solar arrays and thermal control surfaces. As in the case of momentum flux, N_2 is the main carrier of power flux for $\theta < 40$ deg, and H_2 dominates for $\theta > 50$ deg. The kinetic power on the centerline is 3500–4000 W/sr, decreasing to 4–8 W/sr at $\theta = 90$ deg. Total kinetic power and power fractions are listed in Table 4, showing a partitioning among the species that differs somewhat from Table 3 in that H_2 and H contribute more to the power flux than they contribute to thrust. The total kinetic power (here measured as 1007 ± 171 W) should in principle exceed the arcjet thrust power ($1/2 F g_0 I_{sp} = 580$ W from PAC data[1] or 760 ± 230 W from our Table 4) because the thrust is reduced by divergence losses. However, it appears that there is an additional source of error in the power flux, most likely the measured speed, which contributes a v^3 term in Eq. (8).

Table 4 Kinetic power flux determined by mass spectrometry at nominal flow (46.4 mg/s)

Species	Power, W	Power fraction
N_2	716 ± 122	0.711
N	105 ± 18	0.104
H_2	151 ± 26	0.150
H	35 ± 6	0.035
Total	1007 ± 171	1.000

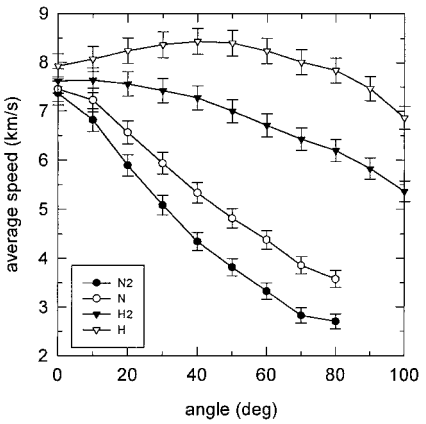

Fig. 11 Average speed vs angle for N_2, N, H_2, and H.

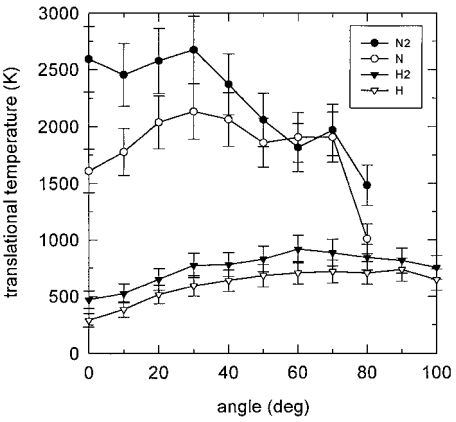

Fig. 12 Translational temperature vs angle for N_2, N, H_2, and H.

The average speed is plotted as a function of angle in Fig. 11, indicating that the velocity slip between N_2 and H_2 is only 0.2 km/s at $\theta = 0$ deg, but the slip increases to 3 km/s at $\theta = 80$ deg. The average speed of N_2 is 7.5 km/s on the centerline and decreases to 2.5 km/s at $\theta = 80$ deg. Changing from nominal flow to high flow causes the average speed for each species to fall off more rapidly with angle. Translational temperature is plotted as a function of angle in Fig. 12, showing values in the range of 1500–2500 K for N_2 and N and 300–900 K for H_2 and H at nominal flow. The N_2 speed distribution is actually narrower than that of H_2 (Figs. 6 and 7), but because they have approximately the same average speed, the N_2 temperature is five to six times higher than the H_2 temperature. Changing from nominal flow to high flow has the effect of lowering the translational temperature, particularly at angles away from centerline.

Conclusions

An investigation of the chemical composition and flow properties of an arcjet thruster plume was performed using molecular beam mass spectrometry with simulated hydrazine propellant. Electron-impact ionization at 20 eV allows H and N atoms in the plume to be detected with minimal interference from dissociative ionization of the parent molecules. Dissociation fractions of N_2 and H_2 are 11 and 14% at the nominal flow rate of 46.4 mg/s and 1660 W of input power. Absolute mass fluxes for N_2, N, H_2, and H are obtained by normalizing the measured relative flux distributions to the total mass flow rate, which together with the speed distributions measured by TOF gives the momentum flux, kinetic power flux, average speed, and translational temperature for each species. Although the average speed is 7.5 km/s near the centerline, the N_2 and N atom speeds decrease quickly with angle, as one would expect based on the rated specific impulse of 514 s. The angular distributions of H_2 and H are much broader than those of N_2 and N, which we interpret as resulting from collisions between light and heavy species, where the light species undergoes a greater deflection and is scattered away from the centerline.

As reported in a separate study,[4] the DSMC calculations at zero background pressure are in very good agreement with the data reported here for the heavy species (N_2 and N), whereas for the light species (H_2 and H), the differences between the experiment and the prediction are indicative of perturbations by the finite background pressure. Average speeds measured for N_2, N, and H_2 are within 0.5 km/s of the prediction at all angles, and for H the agreement is within 0.8 km/s. The measured angular distributions for H_2 and H are somewhat broader than the DSMC results, evidently as a consequence of collisions with the background gas, whereas the N_2 and N angular distributions are very well predicted by the model, consistent with our expectation of a minimal effect by the background.

Acknowledgments

The authors wish to acknowledge the contributions made by L. J. Ortega, M. D. Worshum, E. W. Fournier, M. W. Crofton, and R. B. Cohen at The Aerospace Corporation. Also providing key support were D. M. Zube, J. E. English, and S. Crook of PRIMEX Aerospace Company.

References

[1]Smith, R. D., Roberts, C. R., Aadland, R. S., Lichtin, D. A., and Davies, K., "Flight Qualification of the 1.8 kW MR-509 Hydrazine Arcjet System," International Electric Propulsion Conf., IEPC Paper 97-081, Cleveland, OH, Aug. 1997.

[2]Zube, D. M., Fye, D., Masuda, I., and Gotoh, Y., "Low Bus Voltage Hydrazine Arcjet System for Geostationary Satellites," AIAA Paper 98-3631, July 1998.

[3]Crofton, M. W., Moore, T. A., Boyd, I. D., Masuda, I., and Gotoh, Y., "Near-Field Measurement and Modeling Results for a Flight-Type Arcjet: NH and H Atom," International Electric Propulsion Conf., IEPC Papers 99-042 and 99-048, Kitakyushu, Japan, Oct. 1999.

[4]Nelson, D. A., Masuda, I., and Gotoh, Y., "A Simplified Model for Prediction of Arcjet Plumes," International Electric Propulsion Conf., IEPC Paper 99-043, Kitakyushu, Japan, Oct. 1999.

[5]Pollard, J. E., "Arcjet Plume Studies Using Molecular Beam Mass Spectrometry," International Electric Propulsion Conf., IEPC Paper 93-132, Seattle, WA, Sept. 1993.

[6]Morren, W. E., and Lichon, P. J., "Low-Power Arcjet Test Facility Impacts," AIAA Paper 92-3532, July 1992.

[7]Anderson, J. B., Andres, R. P., and Fenn, J. B., "Supersonic Nozzle Beams," *Advances in Chemical Physics*, edited by J. Ross, 1st ed., Vol. 10, Interscience, New York, 1966, pp. 292–304.

[8]Levine, R. D., and Bernstein, R. B., *Molecular Reaction Dynamics and Chemical Reactivity*, 1st ed., Oxford Univ. Press, New York, 1987, p. 84.

[9]Anderson, J. B., and Fenn, J. B., "Velocity Distributions in Molecular Beams from Nozzle Sources," *Physics of Fluids*, Vol. 8, No. 5, 1965, pp. 780–787.

[10]Pauly, H., and Toennies, J. P., "Beam Experiments at Thermal Energies," *Methods of Experimental Physics*, edited by L. Marton, 1st ed., Vol. 7A, Academic Press, New York, 1968, pp. 238–241.

[11]Kieffer, L. J., "Low-Energy Electron-Collision Cross Section Data," *Atomic Data*, Vol. 1, No. 1, 1969, pp. 19–89.

[12]Abuaf, N., Anderson, J. B., Andres, R. P., Fenn, J. B., and Miller, D. R., "Studies of Low Density Supersonic Jets," *Rarefied Gas Dynamics*, edited by C. L. Brundin, 1st ed., Vol. 2, Academic Press, New York, 1967, pp. 1317–1336.

I. D. Boyd
Associate Editor